

A major purpose of the Technical Information Center is to provide the broadest dissemination possible of information contained in DOE's Research and Development Reports to business, industry, the academic community, and federal, state and local governments.

Although portions of this report are not reproducible, it is being made available in microfiche to facilitate the availability of those parts of the document which are legible.

LA-UR--87-2856

DE87 014754

TITLE LONG-RANGE PULSELENGTH SCALING OF 351nm LASER DAMAGE THRESHOLDS

AUTHOR(S) S. R. Foltyn, CLS-6
L. John Jolin, CLS-6

SUBMITTED TO Proceedings: 1986 Boulder Damage Symposium

DISCLAIMER

This report was prepared as an account of work sponsored by an agency of the United States Government. Neither the United States Government nor any agency thereof, nor any of their employees, makes any warranty, express or implied, or assumes any legal liability or responsibility for the accuracy, completeness, or usefulness of any information, apparatus, product, or process disclosed, or represents that its use would not infringe privately owned rights. Reference herein to any specific commercial product, process, or service by trade name, trademark, manufacturer, or otherwise does not necessarily constitute or imply its endorsement, recommendation, or favoring by the United States Government or any agency thereof. The views and opinions of authors expressed herein do not necessarily state or reflect those of the United States Government or any agency thereof.

By acceptance of this article the publisher recognizes that the U.S. Government retains a nonexclusive, royalty-free license to publish or reproduce the published form of this contribution or to allow others to do so, for U.S. Government purposes.

The Los Alamos National Laboratory requests that the publisher identify this article as work performed under the auspices of the U.S. Department of Energy.

MASTER
Los Alamos Los Alamos National Laboratory
Los Alamos, New Mexico 87545

DISTRIBUTION OF THIS DOCUMENT IS UNLIMITED *mr*

Long-Range Pulselength Scaling of 351nm Laser Damage Thresholds

S. R. Foltyn and L. John Jolin

Los Alamos National Laboratory
CLS-6 MS-J564
Los Alamos, NM 87545

In a series of experiments incorporating 351nm pulselengths of 9, 26, 54, and 625ns, it was found that laser damage thresholds increased as (pulselength)^x, and that the exponent averaged 0.36 and ranged, for different samples, from 0.23-0.48. Similar results were obtained when only catastrophic damage was considered. Samples included Al₂O₃/SiO₂ in both AR and HR multilayers, HR's of Sc₂O₃/SiO₂ and HfO₂/SiO₂, and an Al-on-pyrex mirror; 9ns thresholds were between 0.2-5.6 J/cm².

When these data were compared with a wide range of other results - for wavelengths from 0.25 to 10.6 microns and pulselengths down to 4ps - a remarkably consistent picture emerged. Damage thresholds, on average, increase approximately as the cube-root of pulselength from picoseconds to nearly a microsecond, and do so regardless of wavelength or material under test.

Key words: Al₂O₃; catastrophic damage; coating defects; damage thresholds; excimer lasers; HfO₂; multilayer dielectric coatings; pulselength scaling; Sc₂O₃; XeF lasers.

1. Introduction

Scaling of optical damage thresholds over a long pulselength range has become increasingly important with the continued development of electron-beam pumped excimer lasers. Pulselengths of e-beam devices (0.5-2 μ s) are about two orders of magnitude longer than of avalanche discharge lasers typically used in the laboratory, yet the latter provide the only reliable means to obtain high quality, statistically significant optical damage data.

In order to develop a capability to predict microsecond thresholds from 10 nanosecond data, a representative set of 351nm optical coatings was tested at pulselengths from 9ns to 625ns. In addition to measurement of threshold scale factors, issues such as the functional form of pulselength scaling, scaling for catastrophic damage versus microscopic damage, and the influence of pulselength on defect density were studied.

A wealth of experimental pulselength scaling data has appeared in the literature over the past fifteen years. Since the present results cover a previously unexplored region of long pulselength and short wavelength, a survey of past results was conducted to determine whether pulselength scaling under present conditions differs from that obtained previously.

2. Experimental Conditions

2.1. Laser Operating Conditions

Table 1. contains a listing of laser sources and relevant operating parameters for the four pulselengths employed in this work. The 9ns measurements were made in a production test facility under standard conditions for excimer-based testing at Los Alamos. The longer pulselength work was conducted in an adjoining laboratory using a similar hardware configuration and methodology. The newer excimer laser in this facility was equipped with high-energy electrodes, producing a 26ns pulselength and a more nearly square beam cross section. Increasing optical feedback from 4% to values between 50% and 90% more than doubled the pulselength and, in the case of 50% feedback, doubled the output energy to 350mJ. For these tests, however, 90% was found to provide the smoothest temporal shape with sufficient energy (100-150mJ).

The longest pulse was obtained with a commercial flashlamp-pumped dye laser and second-harmonic generator. LD-700 in methanol provided the fundamental frequency, which was doubled to 355nm in an angle-tuned ADP crystal. Although the pulse repetition rate of this laser was substantially lower than that used for the other tests, previous results [1] at 308nm have demonstrated that thresholds are unaffected by prf variations below 250pps.

Temporal profiles for each pulselength are shown in figure 1.

Table 1. Sources and Test Conditions

Pulselength ^a	Laser	Spotsize ^b	Wavelength	PRF
9ns	XeF excimer (Lumonics 861)	0.44mm	351nm	35pps
26ns	XeF excimer (Lumonics 861T-4)	0.71mm	351nm	35pps
54ns	XeF excimer (Lumonics 861T-4) ^c	0.72mm	351nm	35pps
625ns	Frequency-doubled dye (Candela UV-500)	0.44mm	355nm	0.5pps

^a FWHM.

^b Mean diameter @ 1/e² amplitude.

^c With 10% output coupling.

2.2. Test Samples

Six coating types were chosen for these experiments to represent a realistic cross section of 351nm optics. Multilayer dielectric reflectors included a narrow bandwidth design incorporating Al_2O_3 and SiO_2 , plus $\text{Sc}_2\text{O}_3/\text{SiO}_2$, and two broadband examples of $\text{HfO}_2/\text{SiO}_2$. Designs were all-quarterwave with a halfwave overcoat, and employed a sufficient number of layers to achieve 99% reflectance at 351nm. In addition, an $\text{Al}_2\text{O}_3/\text{SiO}_2$ AR coating was evaluated, as was a MgF_2 -overcoated Al mirror. Substrates for the dielectric films were fused silica; the Al coating was deposited on pyrex.

2.3. Test Methodology

Each test involved the generation of a damage probability plot typically incorporating data from several samples; between 50 and 400 sites were tested on each coating type at each pulselength. Three methods were employed to scale results obtained at different pulselengths:

Method 1. Comparison of the 0% intercepts of linear regression fits to the probability data;

Method 2. Comparison of the lowest damaging fluence values;

Method 3. Comparison of the lowest fluence values producing catastrophic damage.

3. Results and Discussion

Short-pulse damage thresholds from 0.2 to 5.6 J/cm² were measured for the six sample types. Perhaps 95% of the 351nm optics tested at Los Alamos fall within this range. Thresholds were typical for the antireflection coating and the Al mirror, while the Sc_2O_3 reflector was somewhat above average and the Al_2O_3 reflector was a very weak example of this coating type. One reflector using HfO_2 was near the top of its normal range, the other was at the bottom. Measured 9ns thresholds and scale factors (ratios of 625ns to 9ns thresholds) appear in table 2.

Scale factors are seen to vary somewhat with method of comparison. Since the variations are largest for coating types with shallow probability curves, they can likely be attributed to uncertainty in the determination of individual thresholds. In order to reduce the effect of these uncertainties and also to more accurately represent the process normally used to extract a threshold from probability data, scale factors in the discussion that follows are average values from Methods 1 and 2. These methods involve microscopic damage events; considering only catastrophic damage (Method 3) gives similar results.

Table 2. Damage Threshold Scale Factors: 9ns - 625ns

Coating Materials	9ns Damage Threshold	Scale Factor for 625ns Threshold		
		Method 1	Method 2	Method 3
Sc ₂ O ₃ /SiO ₂ (HR) ^a	5.6 J/cm ²	5.0	7.5	6.7
HfO ₂ /SiO ₂ (HR) ^a	3.7 J/cm ²	2.7	2.8	4.3
Al ₂ O ₃ /SiO ₂ (AR) ^b	1.5 J/cm ²	4.2	5.4	---
HfO ₂ /SiO ₂ (HR) ^c	0.7 J/cm ²	5.6	4.7	4.2
Al ₂ O ₃ /SiO ₂ (HR) ^b	0.5 J/cm ²	6.6	9.0	3.7
Al on pyrex ^d	0.2 J/cm ²	2.4	2.9	2.9

Method 1. Intercept of linear regression fit.
Method 2. Lowest damaging fluence.
Method 3. Lowest fluence for catastrophic damage.

- a. Interoptics, Ltd.
b. Eroomer Research Corp.
c. Laser Optics, Inc.
d. Newport Corp.

Damage thresholds at all four pulselengths are summarized in figure 2. Power-law fits indicate that threshold improvement with pulselength ranges, for different sample types, from a fourth-root to a square-root dependence. There is no correlation between these scaling rates and any readily apparent or measurable property of the coatings such as index, threshold, bandgap [2], or reflectance. A particularly good illustration of this is the two examples of HfO₂/SiO₂, which are essentially identical designs produced by different vendors, and which have markedly different scaling behavior.

Another observed difference between coating types was a change in the density of damage-prone defects for 9ns versus 625ns pulses. Since the test spotsize for these two pulselengths was identical, slopes of the probability curves are directly related to defect density [3]. For the Al₂O₃/SiO₂ reflector of figure 3, slopes are nearly identical after fluence scaling; this implies that the defect density is the same for both pulselengths. For the antireflection coating of the same materials (fig. 4) they are notably different, indicating a higher density for the shorter pulselength. Half of the six coating types exhibited no density variation with pulselength while, for the other half, short-pulse defect densities were 2-6x higher. Again, these variations in defect density were

uncorrelated with scaling rates or other readily apparent coating properties.

4. Comparison with Other Data

Figure 5 is a compilation of published scaling results at 351-355nm with thresholds normalized to 10ns. In addition to the present work, three independent data sets are included:

1. A quarterwave single layer tested at 355nm with 20ps and 27ns pulselengths [4];
2. Eight materials in various thickness single-layers tested at 353nm with 5ns and 15ns pulselengths [5];
3. Five HR and four AR coatings tested at 351 or 355nm with pulselengths of 0.6, 1, 5, and 9ns [6].

The results are remarkably consistent. From 0.6ns to 625ns average scaling is $t^{0.32}$. For the Walker, Rainer, and present results, both fast (0.5-0.8) and slow (0.0-0.2) scaling exponents were observed.

Extending this comparison further is a listing, in table 3, of test data covering wavelengths from 248nm to 10.6um and more than five decades in pulselength [4-14]. Again, the results are remarkably consistent. While scaling exponents for individual tests vary widely, the average scaling rate has a nearly constant value from 4ps to 625ns. Thresholds improve as $t^{0.3-0.4}$ for picosecond pulses, and continue to do so for pulselengths up to a microsecond. It is apparent from this compilation that cube-root scaling - as opposed to square-root - is a more accurate rule of thumb for the effect of pulselength on damage threshold.

One final observation is illustrated by the 20ps datum of Newnam in figure 5. Although this point falls within the error bars for an individual measurement, its position relative to the other data suggests an inflection at about 1ns. Such inflections - as well as other forms of non-power law behavior - have been predicted in both inclusion [15-17] and avalanche [18] models of damage. Typically the inflection or curvature is invoked to reconcile t^0 dependence for short pulselengths and t^1 dependence for long ones. From picosecond to microsecond pulselengths, this transition from a constant fluence regime to one in which the damaging field is constant is experimentally unsupported: A simple power law relationship provides a good description of experimental results over the entire range.

Table 3. Pulselength Scaling Comparison

Reference		Wavelength (μm)	Pulselength Range (ns)	Scaling Exponent ^a Range	Average
Soileau	[7]	1.05	0.004 - 0.008	0.0 - 0.5	0.3
Bliss	[8]	0.69	0.020 - 23	0.4 - 0.5	0.4
Newnam	[4]	0.36	0.020 - 27		0.2
Soileau	[7]	0.53	0.03 - 0.15	0.1 - 0.9	0.7
Deaton	[9]	0.27	0.1 - 0.7	0.0 - 0.7	0.3
Milam	[10]	1.06	0.17 - 3.2	0.3 - 0.5	0.4
Lowdermilk	[11]	1.06	0.17 - 3.5	0.0 - 0.5	0.3
Rainer	[6]	0.36	0.6 - 9	0.1 - 0.5	0.3
Milam	[12]	1.06	1 - 9	0.3 - 0.6	0.6
Newnam	[13]	10.6	1.7 - 65	0.2 - 0.3	0.3
Walker	[5]	0.27	5 - 15	0.0 - 1.0	0.5
		0.36	5 - 15	0.0 - 0.8	0.5
		0.53	5 - 15	0.0 - 0.8	0.5
		1.06	5 - 15	0.0 - 0.7	0.3
Boyar	[14]	0.25	10 - 38	0.2 - 0.5	0.3
This Work		0.35	9 - 625	0.2 - 0.5	0.4

^a The value of x in the relationship: threshold fluence \propto (pulselength) ^{x}

5. Conclusions

In testing six 351nm coating types, damage thresholds were found to increase - from 9ns to 625ns - at a rate varying from the fourth-root of pulselength to the square-root. The increase was the same for both catastrophic and microscopic damage, and was not correlated with any readily apparent optical or physical property of the coatings.

A review of published pulselength scaling data indicates that the present work is consistent with earlier findings: From the uv to the mid-in, and from picoseconds to a microsecond, fluence thresholds improve on

average as the cube-root of pulselength, while individual samples may scale quite differently.

This wide range of scaling rates severely limits the ability to accurately predict individual long-pulse thresholds from short-pulse data. As an example, the present results indicate that a 3 J/cm^2 coating at 9ns can be expected to have a threshold anywhere between 9 and 29 J/cm^2 at 1us.

The authors wish to acknowledge the assistance of Bill Leamon who produced most of the 9ns test results and also contributed to the testing at longer pulselengths.

6. References

- [1] Foltyn, S.R. Optical damage research at Los Alamos. Los Alamos Report LA-UR-86-3446. 1986 November.
- [2] Brawer, S.; Smith, W.L. Theory of laser damage in dielectric solids. Nat. Bur. Stand. (U.S.) Spec. Publ. 541; 1978. 303 p.
- [3] Foltyn, S.R. Spotsizes effects in laser damage testing. Nat. Bur. Stand. (U.S.) Spec. Publ. 669; 1982. 368 p.
- [4] Newnam, B.E.; Gill, D.H. Ultraviolet damage resistance of laser coatings. Nat. Bur. Stand. (U.S.) Spec. Publ. 541; 1978. 190 p.
- [5] Walker, T.W.; Guenther, A.H.; Nielsen, P.E. Pulsed laser-induced damage to thin-film optical coatings -- Part I: Experimental. IEEE J. Quant. Elect. QE-17(10): 2041-2052; 1981 October.
- [6] Rainer, F.; Vercimak, C.L.; Milam, D.; Carniglia, C.K.; Tuttle Hart, T. Measurements of the dependence of damage thresholds on laser wavelength, pulse duration and film thickness. Nat. Bur. Stand. (U.S.) Spec. Publ. 688; 1983. 268 p.
- [7] Soileau, M.J.; Williams, W.E.; Van Stryland, E.W.; Boggess, T.F.; Smirl, A.L. Temporal dependence of laser-induced breakdown in NaCl and SiO₂. Nat. Bur. Stand. (U.S.) Spec. Publ. 669; 1982. 387 p.
- [8] Bliss, E.S.; Milam, D. Laser induced damage to mirrors at two pulse durations. Nat. Bur. Stand. (U.S.) Spec. Publ. 372; 1972. 108 p.
- [9] Deaton, T.F.; Smith, W.L. Laser-induced damage measurements with 266nm pulses. Nat. Bur. Stand. (U.S.) Spec. Publ. 568; 1979. 417 p.
- [10] Milam, D. 1064-nm laser damage thresholds of polished glass surfaces as a function of pulse duration and surface roughness. Nat. Bur. Stand. (U.S.) Spec. Publ. 541; 1978. 164 p.

- [11] Lowdermilk, W.H.; Milam, D.; Rainer, F. Damage to coatings and surfaces by 1.06 μ m pulses. Nat. Bur. Stand. (U.S.) Spec. Publ. 568; 1979. 391 p.
- [12] Milam, D.; Thomas, I.M.; Weinzapfel, C.; Wilder, J.G. Pulse duration dependence of 1064-nm laser damage thresholds of porous silica antireflection coatings on fused silica substrates. Nat. Bur. Stand. (U.S.) Spec. Publ. 727; 1984. 211 p.
- [13] Newnam, B.E.; Nowak, A.V.; Gill, D.H. Short-pulse CO₂ Laser damage studies of NaCl and KCl windows. Nat. Bur. Stand. (U.S.) Spec. Publ. 568; 1979. 209 p.
- [14] Boyer, J. (unpublished work in progress).
- [15] Bliss, E.S. Pulse duration dependence of laser damage mechanisms. Nat. Bur. Stand. (U.S.) Spec. Publ. 341; 1970. 105 p.
- [16] Danileiko, Yu. K.; Manenkov, A.A.; Nechitailo, V.S. The role of absorbing defects in the laser damage of transparent materials. Nat. Bur. Stand. (U.S.) Spec. Publ. 620; 1980. 369 p.
- [17] Lange, M.R.; McIver, J.K. Laser induced damage of a thin film with an absorbing inclusion: thermal considerations of substrates and absorption profiles. Nat. Bur. Stand. (U.S.) Spec. Publ. 688; 1983. 448 p.
- [18] Sparks, M.; Holstein, T.; Warren, R.; Mills, D.L.; Maradudin, A.A.; Sham, L.J.; Loh, E.; King, F. Theory of electron avalanche breakdown in solids. Nat. Bur. Stand. (U.S.) Spec. Publ. 568; 1979. 467 p.

FIGURE CAPTIONS

Figure 1. Oscilloscope traces and FWHM values for each of the pulselengths used in this work.

Figure 2. Damage thresholds at 9, 26, 54, and 625ns pulselengths for six different 351nm coating types. Slopes of the lines, which represent best linear regression fits to the data, indicate that thresholds scale at rates ranging from fourth-root to square-root of the pulselength.

Figure 3. Damage probability plots for the $\text{Al}_2\text{O}_3/\text{SiO}_2$ reflectors at 9ns and - with scaled fluence values - 625ns pulselengths. After scaling, the slopes are nearly identical indicating equal defect densities at each pulselength.

Figure 4. Probability plots for $\text{Al}_2\text{O}_3/\text{SiO}_2$ antireflection coatings. The steeper slope for 9ns indicates a 6x higher density of defects for the shorter pulses.

Figure 5. Results of this work plus three other 351-355nm data sets (refs. 2-4). All thresholds are normalized to 10ns. Symbols represent average scaling for each data set; error bars represent extreme scaling values for each set. Solid line indicates the weighted average scaling for the range 0.6-625ns, which is $t^{0.32}$. The dashed line indicates the slope appropriate for square-root scaling.

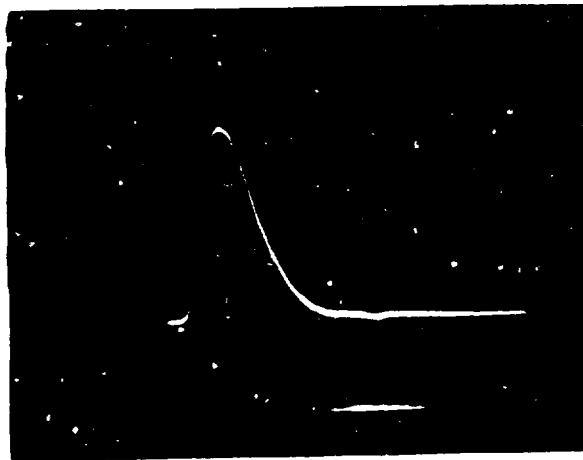
TEMPORAL PROFILES



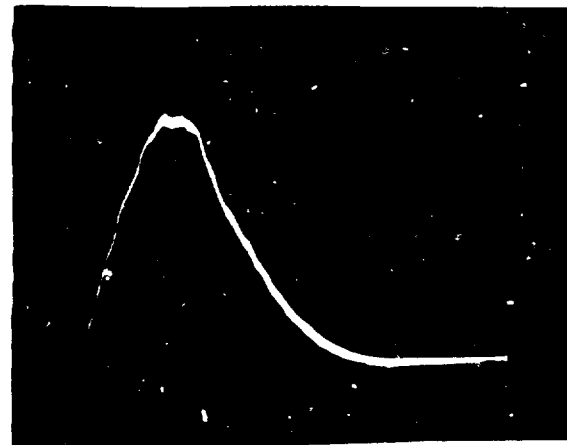
9 ns



54 ns

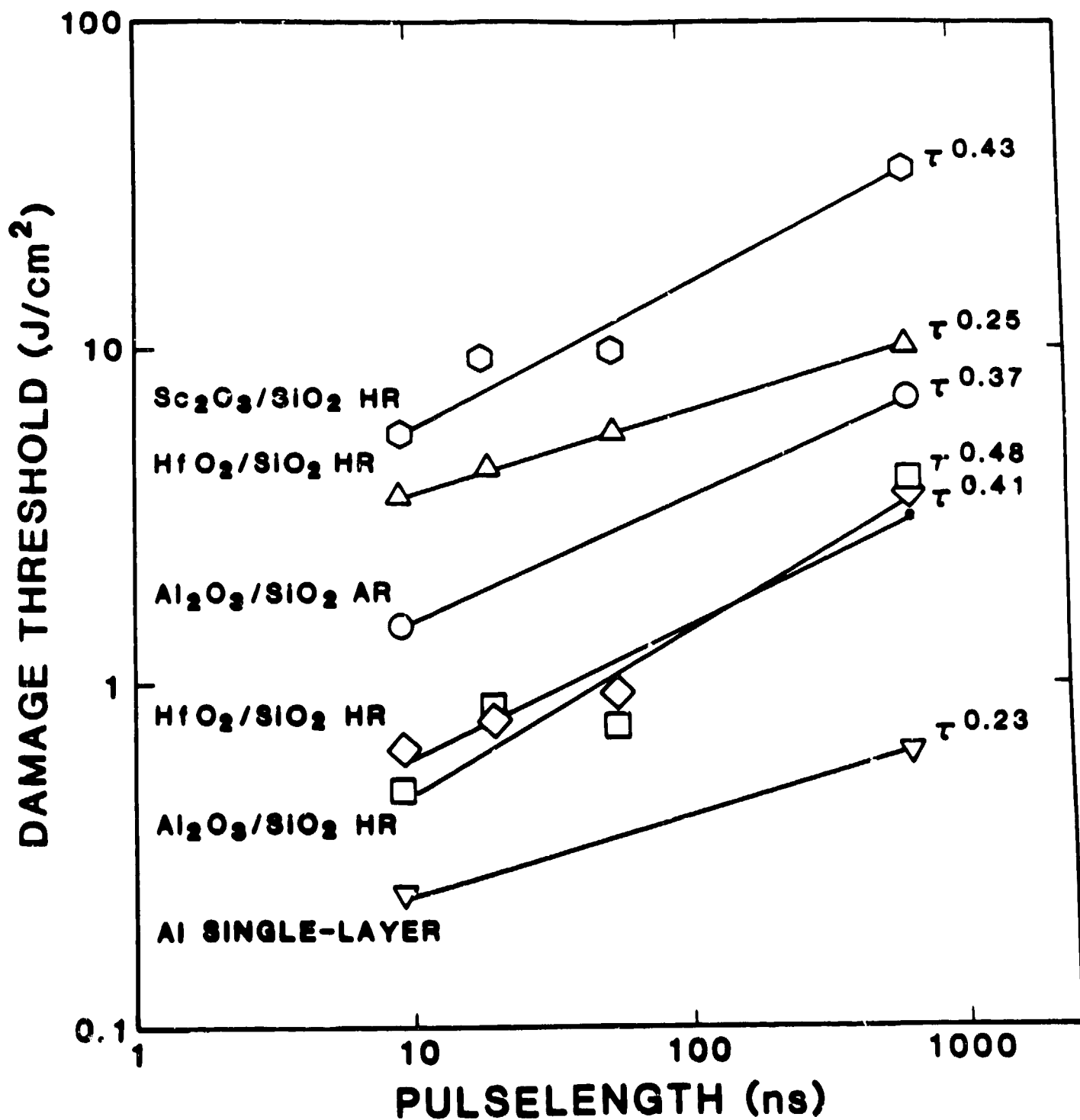


26 ns



625 ns

PULSELENGTH SCALING OF 351/355 nm DAMAGE THRESHOLDS



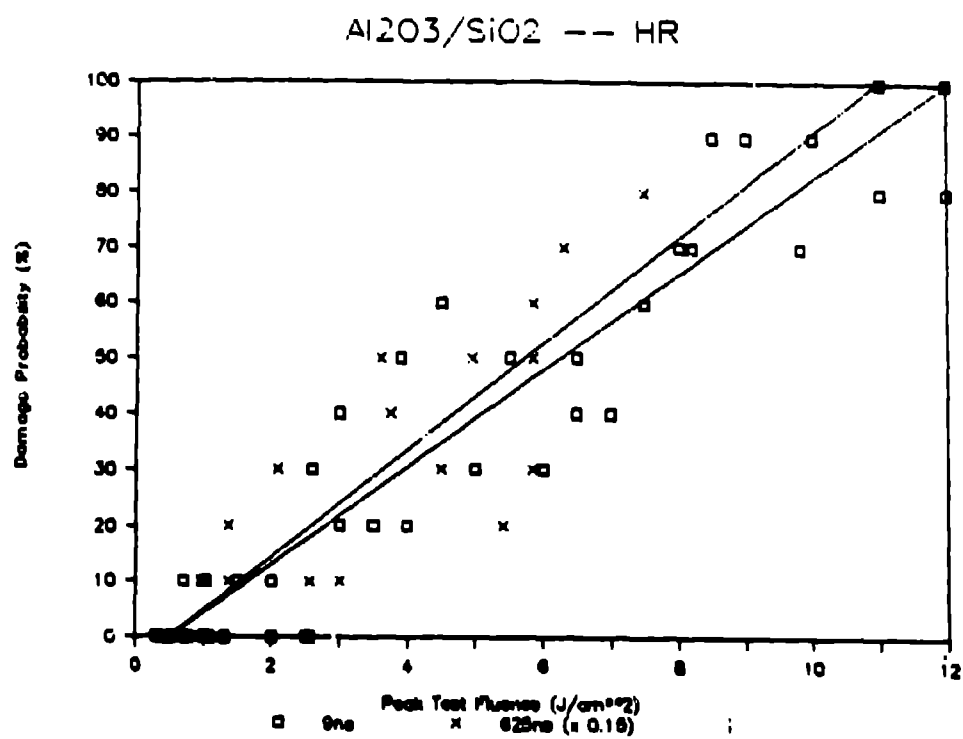


FIG. 3

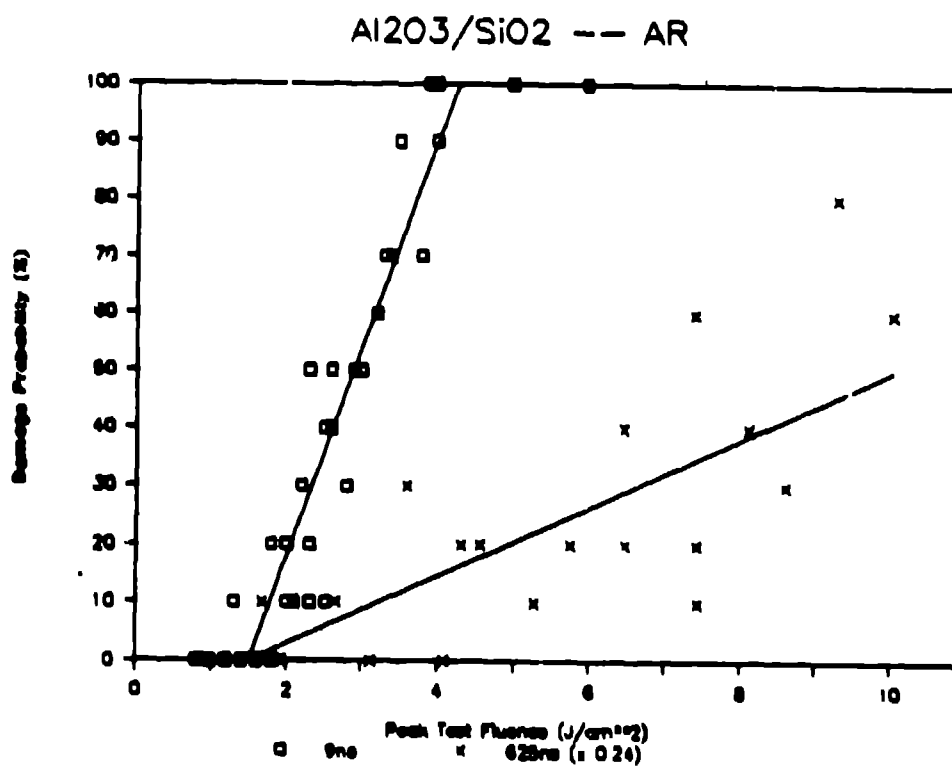


FIG. 4

PULSELENGTH SCALING AT 351-355 nm

